Volume 1 | Number 1 | Jan 2013 | Pages 1–100

Journal of
Materials Chemistry B

Materials for biology and medicine
www.rsc.org/materialsB

ROYAL SOCIETY
OF CHEMISTRY

ROYAL SOCIETY
OF CHEMISTRY

www.rsc.org/materialsB

Use of nucleic acids anchor system to reveal apoferritin modification by cadmium telluride nanoparticles

Jiri Kudr[1,2], Lukas Nejdl[1,2], Sylvie Skalickova[1], Michal Zurek[2], Vedran Milosavljevic[1,2], Renata Kensova[1,2], Branislav Ruttkay-Nedecky[1,2], Pavel Kopel[1,2], David Hynek[1,2], Marie Novotna[1,2], Vojtech Adam[1,2] and Rene Kizek[1,2]

[1]*Department of Chemistry and Biochemistry, Faculty of Agronomy, Mendel University in Brno, Zemedelska 1, CZ-613 00 Brno, Czech Republic, European Union*

[2]*Central European Institute of Technology, Brno University of Technology, Technicka 3058/10, CZ-616 00 Brno, Czech Republic, European Union*

*Corresponding author

Rene Kizek, Department of Chemistry and Biochemistry, Mendel University in Brno, Zemedelska 1, CZ-613 00 Brno, Czech Republic, European Union; E-mail: kizek@sci.muni.cz; phone: +420-5-4513-3350; fax: +420-5-4521-2044

Abstract

The aim of this study was to synthesize CdTe NPs modified apoferritin and examine, if apoferritin is able to accommodate CdTe NPs. Primarily, the thermostability of horse spleen apoferritin was tested and its unfolding at 70 °C was observed. Cadmium telluride nanoparticles (CdTe NPs) were synthesized both within apoferritin protein cage and on its surface. Thermal treatment of apoferritin with CdTe NPs resulted in the aggregation of cores, indicated by changes of absorption spectra and shape of apoferritin tryptophan fluorescence. The apoferritin modified with CdTe NPs was additionally modified with gold nanoparticles and attached to magnetic particles via oligonucleotide using gold affinity to thiol group. This anchor system was used to separate construct using external magnetic field and to analyse the molecules attached to apoferritin.

1. Introduction

Nanoparticles have been attracting a great attention due to their wide potential of application[1], where their different shapes, sizes and compositions enhance a possibility of broad range of their use [2-4]. For nanotechnology and biotechnology applications there is a strong demand on uniformity of nanoparticles properties. However there are still technical challenges regarding preparation of nanoparticles with homogeneous size distribution [5].

Various nanoparticles fabrication methods have been reported [6-8]. It was shown that biomolecules such as protein cages or viruses can serve as a template for the synthesis of nanoparticles [9, 10]. The cages-like proteins are able to bio-mineralize inorganic materials and, then, they can be used as a spatially restricted chemical chamber (nanoreactor). Among all protein cages, apoferritin is favoured for its remarkably stable structure under various acidity and temperature [11, 12]. Apoferritin is an iron storage protein, which is ubiquitous in animals. It is composed of 24 polypeptide subunits. Heavy and light subunits self-assemble into a hollow protein sphere with outer and inner diameters of 12 and 8 nm, respectively [13]. Horse-spleen apoferritin is composed of nearly of 90 % of L-subunit (one tryptophan per L and H subunit at the same position of polypeptide chain). Specific threefold channels at the interface of subunits are responsible for the flow of positive ions to the hollow core. In recent research, apoferritin has been used to synthetize various metal nanoparticles and semiconductor nanocrystals [14-20]. In these cases, aspartate and glutamate on the inner surface were proved to promote the nanoparticles formation [17]. In addition, apoferritin is used in many biomedical applications [21-23].

Magnetic particles have important applications in biochemistry and analytical chemistry such as analyte pre-concentration, separation and identification [24-26]. The target molecule can be recognized by specific magnetic particle surface modification and the magnetic force enables separation of adsorbed target molecule from a complex sample [27, 28]. The modification of

58 magnetic particles with oligonucleotide probe is broadly used for biosensors fabrication and

59 medical applications due to their unique biorecognition properties based on the ability to

60 hybridize target sequence and to eliminate non-specific adsorption [29-33].

61 As it was mentioned above protein cages including apoferritin are broadly used in the field of

62 material science. Therefore, the aim of this study was to synthesize CdTe NPs modified

63 apoferritin and examine, if apoferritin is able to accommodate CdTe NPs. Moreover, we

64 designed the anchor system based on modified magnetic particles to prove apoferritin

65 modification by CdTe NPs. The advantage of the proposed system is not only in synthesis of

66 nanoparticles within the apoferritin cage but also in the possibility to purify this nanoreactor

67 from the unreacted components of the synthesis and moreover to transfer it to desired location

68 by external magnetic field manipulation due to the conjugation with magnetic field responsive

69 particles.

70

2. Material and Methods

2.1. Chemicals

73 Water, cadmium acetate dihydrate, sodium tellurite, sodium borohydride and other chemicals

74 were purchased from Sigma-Aldrich (St. Louis, USA) in ACS purity (chemicals meet the

75 specifications of the American Chemical Society), unless noted otherwise. Apoferritin from

76 equine spleen (0.2 μm filtered) and the oligonucleotides were also purchased from Sigma-

77 Aldrich (St. Louis, USA). Magnetic particles Dynabeads Oligo(dT)$_{25}$ were bought from

78 Thermo Fisher Scientific (Waltham, USA). pH was measured with pH meter WTW (inoLab,

79 Weilheim, Germany).

80

81

82

2.2. The sample preparation

The apoferritin with CdTe NPs (ApoCdTe NPs) was prepared as it follows. The horse spleen apoferritin (20 µl, 7.3 µg.µl^{-1}) was pipetted into water (300 µl). Then, cadmium acetate (20 µl, 20 mM) and ammonium (4.5 µl, 1 M) were added. After shaking (30 min., 37 °C, 500 RPM) on thermomixer (Eppendorf, Hamburg, Germany), sodium tellurite (3.75 µl, 20 mM) was added to the solution (pH 9.5). To obtain the ApoCdTe NPs sample, sodium borohydride was added to the solution, too. The control sample (CdTe NPs sample) was prepared in the same way, instead of apoferritin, 20 µl of water was added. The water solution of apoferritin (0.4 mg.ml^{-1}) was used to compare the ApoCdTe NPs and apoferritin fluorescence and absorption. After incubation (20 h, 60°C, 500 RPM) on thermomixer (Eppendorf, Germany) all samples were filtered using Amicon Ultra-0.5 ml Centrifugal Filters with 50 kDa cut-off (Merck Millipore, Billerica, USA) according to the manufacturer instructions.

2.3. Preparation of gold nanoparticles (Au NPs)

Gold nanoparticles were prepared using citrate method at room temperature according to [34, 35]. Briefly, an aqueous solution of sodium citrate (0.5 ml, 40 mM) was added to a solution of $HAuCl_4 \cdot 3H_2O$ (10 ml, 1 mM). The colour of the solution slowly changed from yellow to violet. Mixture was stirred overnight. The smallest Au NPs from the top layer of the flask were used for apoferritin modification according to the following protocol. The ApoCdTe NPs, CdTe NPs and apoferritin sample (100 µl) were mixed with the Au NPs (10 µl) and incubated (24 h, 500 RPM, 37 °C) on thermomixer (Eppendorf, Germany).

2.4. Preparation of anchor system

Buffers used for isolation step were phosphate buffer I (pH 6.5, 0.1 M NaCl, 0.05 M Na_2HPO_4, and 0.05 M NaH_2PO_4), phosphate buffer II (0.2 M NaCl, 0.1 M Na_2HPO_4, and 0.1

108 M NaH$_2$PO$_4$) and hybridization buffer (100 mM Na$_2$HPO$_4$, 100 mM NaH$_2$PO$_4$, 0.5 M NaCl,

109 0.6 M Guanidium thiocyanate, and 0.15 M Trizma base adjusted using HCl to pH of 7.5). 10

110 µl of resuspended magnetic particles were placed to the magnetic stand and washed 3-times

111 with phosphate buffer I (100 µl). The magnetic particles were resuspended in the solution

112 containing hybridization buffer (10 µl) and oligonucleotide with polyadenine terminus (10 µl,

113 100 µg.ml^{-1}, 5' TCTGCATTCCAGATGGGAGCATGAGATGAAAAA). Subsequently, this

114 solution was incubated (30 min., 500 RPM, 37 °C) on thermomixer (Eppendorf, Germany)

115 and the particles were washed with phosphate buffer I (100 µl) in order to remove unattached

116 oligonucleotide. The particles were then resuspended in solution containing hybridization

117 buffer (10 µl) and thiolated oligonucleotide (10 µl, 100 µg.ml^{-1},

118 5'CATCTCATGCTCCCATCTGGAATGCAGA-SH). After the incubation (30 min., 500

119 RPM, 37 °C), unbounded oligonucleotide were washed away. The result of preparation was

120 the modified magnetic particles without any fluid. The prepared construct was used to anchor

121 the gold modified ApoCdTe NPs, apoferritin and CdTe NPs samples.

122 The samples with different ApoCdTe NPs concentrations and modified by Au NPs were

123 obtained by diluting the stock solution of ApoCdTe NPs with water in different ratios

124 (undilluted ApoCdTe NPs stock solution, 1:1, 1:3, 1:7, 1:15 and 1:39). The gold modified

125 apoferritin sample (5 µl) and CdTe NPs sample mixed with Au NPs (5 µl) were also mixed

126 with water (35 µl) and used as controls for cadmium detection after separation conducted by

127 anchor system. In addition, these samples (40 µl) were mixed with the prepared modified

128 magnetic particles and incubated (1h, 25 °C, 500 RPM). Subsequently the magnetic particles

129 were washed with phosphate buffer I (100 µl) and the phosphate buffer II was added (10 µl)

130 in order to split the hybridized oligonucleotides. The magnetic particles were immobilized by

131 magnetic field and the supernatants were analysed using atomic absorption spectrometry

132 (AAS).

133

134 *2.5. Instrumentation*

135 Absorption and fluorescence spectra were measured using Infinite 200 PRO multimode reader

136 with top heating (Tecan, Männedorf, Switzerland). Gel electrophoresis was performed using

137 PowerPac Universal Power Supply (Bio-Rad, Hercules, USA). Average current levels were

138 obtained using Scanning electrochemical microscope 920C (CH Instruments, Austin, USA).

139 Spectro Xepos (Spectro Analytical Instruments, Kleve, Germany) was used to measure X-ray

140 fluorescence spectra. Determination of cadmium was carried out on 280Z Agilent

141 Technologies atomic absorption spectrometer (Agilent, Santa Clara, USA) with

142 electrothermal atomization and Zeeman background correction. Average particle size and size

143 distribution were determined by quasielastic laser light scattering with Malvern zetasizer

144 Nano-ZS (Malvern Instruments Ltd., Worcestershire, U.K.).

145

146 *2.6. Apoferritin thermostability*

147 Unfolding of apoferritin was monitored spectrophotometrically using a computer-controlled

148 Peltier thermostat (Labortechnik, Wasserburg, Germany). The sample (35 μg.ml^{-1}) was

149 incubated at different temperatures for 5 min and thereafter absorbance was measured at 230

150 nm. Changes in sample absorbance were recorded using a spectrophotometer Specord S600

151 with a diode detector (Analytik Jena, Jena, Germany). Thermostability of apoferritin was also

152 tested using gel electrophoresis. The solution of apoferritin (35 μg.ml^{-1}) was shaken (500

153 RPM) and heated with thermomixer. The samples (10 μl) were removed from solution during

154 heating when the temperature reached 30, 35, 40, 45, 50, 55, 60, 65, 70 and 75 °C for 5

155 minutes. These samples were further analysed by native (non-denaturing) polyacrylamide gel

156 electrophoresis (native-PAGE).

157

158 *2.7. Non-Denaturing Polyacrylamide Gel Electrophoresis*

159 The samples were analysed in 6% non-denaturing PAGE in 60 mM HEPES and 40 mM

160 imidazole pH 7.4 buffer as described by Kilic et al. [36]. Briefly, the samples (10 µl) were

161 mixed with 2 µl of 30% glycerol. The gels (2.4 ml of Acrylamide/Bis-acrylamide 30%

162 solution, 9.6 ml of running buffer, 9.96 µl of N,N,N′,N′-Tetramethylethylenediamine and 60

163 µl of Ammonium persulfate) were run at 10 mA for 2 hours (30 minutes for apoferritin

164 thermostability experiment) and were stained with Coomassie Brilliant Blue R stain.

165

166 *2.8. The scanning electrochemical microscope measurements*

167 Scanning electrochemical microscope (SECM) consisted of 100 mm measuring platinum disc

168 probe electrode with potential of +0.2 V. During the scanning, particles were attached to the

169 conducting substrate plate coated with gold via magnetic force from neodymium magnet.

170 Working distance of platinum measuring electrode was set to 20 µm above the surface. The

171 mixture consisted of 5 % ferrocene in methanol, mixed in ratio 1:1 ratio with 0.05 % KCl

172 water dilution (v/v).

173

174 *2.9. Stern-Volmer constant*

175 Fluorescence spectra (excitation wavelength 400 nm) of CdTe NPs (emission wavelength 600

176 nm) QDs without any capping agent (50 µl) were measured in the presence of 0, 0.3, 0.6, 0.8,

177 1.1 and 1.4 µM of apoferritin (5 µl) and also at different temperatures (20, 25, 30, 35 and 40

178 °C). The CdTe NPs fluorescence quenching by apoferritin can be described by Stern-Volmer

179 equation:

180
$$\frac{F_0}{F} = 1 + k_q \tau_0 [Q] = 1 + K_{SV}[Q]$$

181 where F_0 and F are fluorescence intensities of CdTe NPs in the absence and presence of

182 apoferritin quencher, respectively, k_q is biomolecular quenching constant, τ_0 is lifetime of the

183 fluorophore without quencher, *[Q]* is the concentration of the quencher and K_{SV} is the Stern-

184 Volmer quenching constant [37]. Quenching constant K_{SV} was calculated by the linear

185 regression of a plot of *(F_0-F)/F* against *[Q]* [38].

186

187 **3. Results and discussion**

188 *3.1. The synthesis of CdTe NPs within apoferritin*

189 The H subunits (represents 10 – 15 % of horse spleen apoferritin) include the ferroxidase

190 centre, which is responsible for oxidation of ferrous oxide to ferric oxide and prevents free

191 radicals production. Apoferritin cavity *in vivo* is able to accommodate 4000 iron atoms stored

192 as a mineral ferrihydrite. The hydrophobic fourfold channels represent large energy barrier for

193 divalent and monovalent ions uptake [39]. Apart from that, the hydrophylic threefold channels

194 transfer monovalent and divalent ions into the apoferritin cavity. This ability is broadly used

195 for nanoparticle synthesis within the cavity. As it was previously proved, the apoferritin

196 cavity is able to accommodate several metal ions and inorganic molecules [14, 15, 40]. From these,

197 cadmium ions are used for ferritin and apoferritin crystallization due to its large coordination

198 numbers [41], and are also able to bridge the otherwise repulsive carboxyl groups of opposing

199 aspartate and glutamine side chains [42].

200 Protein contains three intrinsic fluorophores: phenylalanine, tyrosine and tryptophan, which

201 are also responsible for protein absorption at the UV-region. Tryptophan has longer excitation

202 and emission wavelengths and good quantum yield. Due to the fact that phenylalanine has

203 very low quantum yield and tyrosine is often totally quenched when is located near amino or

204 carboxyl group, protein intrinsic fluorescence mostly rises from tryptophan (its indole ring) [37].

205 Changes in tryptophan fluorescence intensity, band shape, wavelength maximum and

206 fluorescence lifetime depend on the tryptophan local environment and are used in various

207 applications such as substrate binding or quencher accessibility [38, 43-45]. Both, the H and L-

208 chains of apoferritin contain single tryptophan residue, so 24 tryptohan residues are presented

209 within apoferritin. Therefore, we monitored apoferritin emission spectra after excitation at

210 230 nm and observed the changes during sample preparations.

211 Preparation of ApoCdTe NPs (apoferritin modified with CdTe NPs) is schematically depicted

212 in Fig. 1A. More precisely, ammonium (4.5 µl, 1M) and cadmium acetate (20 µl, 20 mM)

213 were added to apoferritin solution (0.4 mg.ml^{-1}). Cadmium ions were stabilized by

214 ammonium ions and created positively charged tetraminecadmium ions, which were partly

215 transported to apoferritn cavity [46]. Then sodium tellurite (3.75 µl, 20 mM) was added and

216 tellurite ions were reduced to telluride by addition of sodium borohydride, which resulted in

217 CdTe cores formation. Subsequent heating was applied to allow CdTe cores to aggregate.

218 The individual steps of ApoCdTe NPs synthesis were monitored using UV-Vis and

219 fluorescence spectroscopy to confirm the CdTe NPs creation. The absorption (230–800 nm)

220 and fluorescence spectra (280–480 nm) were measured and compared with two control

221 samples as (i) CdTe NPs solution without any capping agent and apoferritin (CdTe NPs

222 sample), and (ii) apoferritin water solution. The characteristic absorption peak of protein

223 (apoferritin) was observed at 280 nm in the cases of apoferritin solution with cadmium and

224 tellurite ions (A_{280}=0.91 AU) and apoferritin solution (A_{280}=0.86 AU) before addition of

225 NaBH$_4$. No absorption peak was observed in the case of cadmium and tellurite ions solution

226 (Fig. 1B). The fluorescence spectra of all three samples were also measured (Fig. 1C). The

227 emission peaks of apoferritin and apoferritin in the presence of ions were observed at 308 nm.

228 The sample with cadmium and tellurite ions without apoferritin exhibited emission spectra

229 with no peak. In comparison to sample of ions before addition of reducing agent, the

230 absorption maximum of reduced sample increased in the range from 246 nm to 450 nm due to

231 CdTe cores creation (Fig. 1D), which is on good agreement with Han et al. [47]. Absorption

232 spectra of ApoCdTe NPs and apoferritin sample remained nearly the same after reduction

233 process. The emission of ApoCdTe NPs and apoferritin sample were lower by 4 % and 3%

234 respectively, compared to unreduced samples (Fig. 1E). Fluorescence measurement of CdTe

235 NPs sample immediately after reduction revealed no emission peak (excitation wavelength

236 230 nm), but emission maxima was observed at 584 nm when excited at 400 nm (not shown).

237 We assume that the presence of CdTe quantum dots in solution was responsible for this

238 emission maximum. In the next step the samples were heated (20 h, 60 °C, 500 RPM) to

239 encourage aggregation of CdTe NPs according to Khalavka et al. [48]. The measurement of

240 samples absorption spectra after heating step resulted in the increase of ApoCdTe NPs local

241 maxima at 280 nm by 14 % (compared with reduced ApoCdTe NPs sample) and formation of

242 local maxima at 330 nm, although the absorption spectra of apoferritin sample remained

243 nearly the same (Fig. 1F). The similar absorption spectra of nanoparticle within apoferritin

244 were reported for Pd and Cd [16, 49]. Strong decrease in CdTe NPs sample absorption at UV

245 wavelengths was detected after heating and we assume that this is the consequence of bulk

246 CdTe colloids precipitation (Fig. 1F). Although, fluorescence of apoferritin and ApoCdTe

247 NPs sample with the maxima at 306 nm remained the same after incubation, the peak width

248 changed (Fig. 1G). The emission of CdTe NPs was not observed and the mechanism of

249 quenching is discussed afterwards. Xiao et al. determined the interaction of CdTe quantum

250 dots stabilized by mercapropropionic acid with the human serum albumin by the decrease in

251 albumin fluorescence intensity, however quantum dot properties are strongly affected by the

252 capping agent [50]. Peak width at half height of ApoCdTe NPs (calculated as a distance from the

253 front slope of the peak to the back slope of the peak measured at 50% of the maximum peak

254 height) increased by 54 % in comparison with the emission peak before heating and also

255 increased by 30 % in the case of apoferritin solution. After the heating, no emission peak of

256 CdTe NPs sample was observed when excited at 230 nm and the emission peak also

257 disappeared when excited at 400 nm (not shown). Without any capping agent, heating of

258 quantum dots resulted in theirs aggregation.

259 We also calculated the difference spectra. The absorption and fluorescence spectra of

260 apoferritin solution in particular synthesis step were subtracted from the spectra of ApoCdTe

261 NPs sample. The differential absorption spectra highlighted the differences between samples

262 at 300 nm before and after reduction step and the local maxima increase at 330 nm (Fig. 1H).

263 The heating of ApoCdTe NPs sample resulted in difference fluorescence maxima evolving.

264 The differential fluorescence spectra revealed the increasing peak at 350 nm (Fig. 1I). The

265 difference emission of heated ApoCdTe NPs and heated apoferritin increased 3-times in

266 comparison with difference emission of unheated samples.

267 In addition, the thermostability of apoferritin spherical structure was examined using UV-Vis

268 spectrophotometry and gel electrophoresis. UV-Vis absorbance measurement is a simple

269 method used to examine structural changes and formation of complexes [33, 51, 52]. The protein

270 absorption spectra showed the peak at 280 nm due to the absorption of aromatic side chains of

271 phenylalanine, tyrosine, and due to disulphide bonds, which are responsible for the

272 dimerization of apoferritin H-chains, and mostly by tryptophan [53]. The tryptophan and

273 tyrosine content in various proteins remains constant, and therefore this wavelength is

274 commonly used to determine protein concentration in reagentless nondestructive way.

275 External conditions like temperature, pH and ionic strength cause the changes in the protein

276 conformation, which results in change of amino acids exposure to the solvent and the

277 absorption spectra [54-57]. Although the UV absorption spectra of proteins shows only slopes at

278 app. 230 nm, according to Liu et al. [58], it can be used as convenient structural probe to find

279 thermodynamic stability and kinetics of proteins unfolding. The monitoring of absorbance at

280 230 nm (A_{230}) during the heating was used as structural probe for studying of apoferritin. The

281 steady decrease of A_{230} was observed from 30 °C to 76 °C during the heating of apoferritin

solution (Fig. 1J). Absorbances of apoferritin solution at 30 °C and 76 °C were expressed as 100 % and 0 % respectively. The lowest absorbance (A_{230}= 1.28 AU) was measured after solution reached 76 °C, however absorbance of solutions heated to 68 °C and more were nearly the same. We suggest that heating of apoferritin above body temperature resulted in conformation changes of apoferritin subunits and total denaturation at 68 °C was observed, nevertheless substantial reversibility of horse spleen apoferritin denaturation was observed up to a few degrees below denaturation temperature [11]. UV spectra of folded and unfolded protein commonly shows downward peak (UV absorption of unfolded protein is lower) [58].

Unfolding and denaturation of apoferritin was also examined using the native polyacrylamide gel electrophoresis (Fig. 1K). Smears corresponding to release of apoferritin subunits were observed in case of samples heated above 65 °C but it seems to have reached higher intensity at 70 °C. Taking together data from UV absorption and gel electrophoresis, we conclude that spherical structure of apoferritin degrades in temperature above 65 °C. Based on previous results we have chosen 60 °C as a safe temperature for CdTe NPs aggregation in the presence of spherical state of apoferritin. Stefanini et al. (1996) suggests that the horse spleen apoferritin should not be heated to 80 °C to avoid its irreversible denaturation [11]. Our results confirm high thermostability of horse spleen apoferritin, which is consistent with the thermostability of the whole ferritin group as it was determined in the case of ferritin from hyperthermophile *Pyrococcus furiosus*, which is stable up to 120 °C [14].

The average particle sizes and particle size distribution within samples were determined using zetasizer, nevertheless electrochemical methods were suggested to be able to determine nanoparticle sizes (Fig. 1L) [59]. Average CdTe colloid had 295 nm in diameter after heating, although we assume that their size without capping agent is not stable. Average size of spherical apoferritin was found to be 11 nm, which correspond with the commonly accepted size of apoferritin (12 nm). Two main particle fractions were detected in the case of ApoCdTe

307 NPs sample as (i) CdTe colloids with average sizes of 255 nm and (ii) apoferritin modified by

308 CdTe NPs with average diameter of 18 nm.

309 As we observed the quenching of CdTe NPs fluorescence by apoferritin and *vice versa,* we

310 used the calculations of Stern-Volmers constants to elucidate the interaction of CdTe NPs and

311 apoferritin surface. Fluorescence quenching mechanism is usually described as either dynamic

312 or static and can be determined using different temperature dependence [60]. As it is shown in

313 Fig. 1M, calculated Stern-Volmer quenching constants K_{SV} of CdTe NPs are inversely

314 correlated with the increasing temperature. This phenomenon is often observed in the case of

315 static quenching and suggests that the quenching of CdTe NPs is the consequence of theirs

316 binding to the surface of apoferritin, rather than by dynamic collision [61].

317 **Figure 1**

318

319 *3.2. Anchoring of the apoferritin samples*

320 Utilization of the apoferritin cage as a nanoreactor provides variety of advantages, however

321 also the manipulation of such molecule by external stimuli is of an interest mainly to enable

322 the reaction to take place at the desired place and subsequently transfer the product to the site

323 of action. Therefore, an elegant approach of application of magnetic particles can be taken.

324 For this reason, a simple connection using gold nanoparticles and complementary

325 olinucleotides was proposed enabling to simply connect the cage to the magnetic particle and

326 spatially manipulated the nanoreactor.

327 In the following experiments, apoferritin, CdTe NPs and ApoCdTe NPs samples were mixed

328 with the gold nanoparticles (Au NPs). Covalent bond between Au and S is most widely used

329 interaction to achieve stable conjugation between AuNPs and oligonucleotides or proteins

330 containing cystein [62-64]. The citrate capped Au NPs are known as one of the easily synthesized

331 NPs thus are frequently used for biosensors fabrication and biomolecule labelling [65-67]. The

332 exposed citrate is responsible for the negative charge of Au NPs surface [68]. Due to the fact

333 that the apoferritin inner surface has a negative electrostatic potential due to the presence of

334 many acidic amino acids residues, which is important to attracting metal ions from solution

335 during biomineralization, the electrostatic binding between Au NPs and apoferritin (horse

336 spleen apoferritin *pI* is between 4.1–5.5) is impossible in neutral pH [69]. Our concept of

337 apoferritin modification with Au NPs relies on the apoferritin's ability to displace the citrate

338 on nanoparticle surface as a result of direct interaction of amino acids functional group (thiol

339 of cysteine, amine of lysine or imidazole of histidine) with gold surface. The forming of

340 chemical bond between sulphur from apoferritin cystein and gold was previously reported [70].

341 The integrity of apoferritin structure during the CdTe NPs synthesis was examined using gel

342 electrophoresis (Fig. 2A). The apoferritin sample and apoferritin sample after Au NPs

343 modification was run in the gel (Fig. 2A a, e). The band of native apoferritin nanosphere was

344 found to be app. 1 cm from the beginning (Fig. 2A red arrow), which was reported by Kilic et

345 al. under these conditions [71]. The faint band attributed to the dimeric form of apoferritin

346 sphere was also observed (Fig. 2A green arrow), which is in good agreement with Kilic et al.

347 [36]. After apoferritin sample heating (20 h, 60 °C, 500 RPM), the sample was filtered using

348 filter unit with 50 kDa cut off and the filtrate was analysed on PAGE (Fig. 2Ac). There was

349 no apoferritin subunit band detected (both approximately 20 kDa), thus we concluded that the

350 integration of apoferritin was mostly preserved after heating. The ApoCdTe NPs sample was

351 treated in the same way. In Figs. 2Ab, d, and f there are shown ApoCdTe NPs sample after

352 synthesis, its filtrate and ApoCdTe NPs modified by Au NPs. The positions of ApoCdTe NPs

353 sample bands are similar to bands of apoferritin sample. The slight shifts of ApoCdTe NPs

354 bands were observed only. We assume that protein charge was not changed. Therefore, we

355 came to the conclusion that it is the result of CdTe NPs attachment to apoferritin surface and

356 the increase of its hydrodynamic size, as also suggested by particles size distribution and

357 static quenching of CdTe NPs fluorescence by apoferritin (Fig. 1L).

358 In the conclusion, no shifts of bands of apoferritin and ApoCdTe NPs were observed after

359 their modification with gold nanoparticles. The bands intensities of ApoCdTe NPs and

360 ApoCdTe NPs modified with Au NPs are not so well-marked as the apoferritin bands.

361 Thermostability of apoferritin seems to be partly influenced by CdTe NPs presence. Heating

362 (60 °C for 20 h) resulted in apoferritin portion unfolding, indicated by polypeptide aggregates,

363 which cannot go through the native-PAGE and for this reason stacked at the beginning of the

364 gel (Fig. 2A yellow arrow) and they were also not able to go through the filter unit with

365 50 kDa cut-off.

366 Individual steps of nanoconstruct formation were examined using SECM (Fig. 2B). The bare

367 gold plate was first scanned and the average current level was calculated (-0.22 nA). The

368 magnetic particles attached to the gold plate due to magnetic field had average current level

369 -1.65 nA. The oligonucleotide with terminal polyA sequence was hybridized to magnetic

370 particles. This complex was then hybridized to complementary oligonucleotide with thiolated

371 terminus and Au NPs were immobilized on its thiol groups. This part of construct decreased

372 the reduction signal by 0.96 nA to -2.61 nA. The construct extended by apoferritin resulted in

373 the decrease of signal by 3.12 nA to -5.73 nA, so the apoferritin addition increased the amount

374 of reducible substances by 120 %. The presence of CdTe NPs within apoferritin cavity and on

375 the apoferritin surface decreased the average current level four-times to -22.90 nA. The

376 SECM record of ApoCdTe NPs immobilized on the surface of gold electrode using anchor

377 system and applying of external magnetic field is shown in Fig. 2C.

378

379

380

381 **Figure 2**

382

383 *3.3. The presence of CdTe nanoparticles within apoferritin*

384 The Au NPs were added to the apoferritin, CdTe NPs and ApoCdTe NPs samples. After the

385 incubation of samples with the Au NPs, we used the anchor system to capture the Au NPs and

386 molecules attached to them (Fig. 3A). Oligonucleotide probes with terminal AAA sequence

387 were hybridized to magnetic particles with TTT sequence bound to theirs surface. Second

388 probes with thiol groups were hybridized to the first one and together formed a system

389 capable of anchoring gold modified biomolecules. Different concentrations of ApoCdTe NPs

390 sample modified with Au NPs were added to oligonucleotides with attached magnetic

391 particles. CdTe NPs solution was added to magnetic particle as a control. After incubation

392 (1 h, 25 °C), these constructs were separated from solution of unattached molecules applying

393 external magnetic field. Subsequently, the hybridized oligonucleotides in constructs were

394 disrupted due to chemical denaturation and the magnetic particles were removed from the

395 samples. Finally, the samples were analysed using atomic absorption spectrometry (AAS). No

396 trace of cadmium was detected in control samples. It means that no CdTe NPs were modified

397 by Au NPs and anchored. Apart from that, ApoCdTe NPs was successfully modified by Au

398 NPs and attached to the anchor system. The dependence of detected amount of total cadmium

399 on the volume of ApoCdTe NPs applied to the anchor system proved the modification of

400 apoferritin by CdTe NPs and it is shown in Fig. 3B. Further, we calculated that ratio of

401 detected cadmium to one apoferritin anchored molecule as it was 2700 : 1. The sizes and sizes

402 distributions of gold nanoparticles used for apoferritin modification and particles separated

403 from ApoCdTe NPs solution were measured and compared with the size distribution of the

404 particles presented within the ApoCdTe NPs solution (Fig. 3C). We observed that gold

405 nanoparticles with average diameter of 4 nm exhibited a broad size distribution from 1 to

406 8 nm. In this case we suggest that the gold nanoparticles aggregation and cluster formation is

407 partly responsible for this size distribution and also for the presence of second size

408 distribution peak from 10 to 120 nm. The size distribution of ApoCdTe NPs sample consisted

409 of two peaks. The first peak, at app. 18 nm, was assigned to the apoferritin with CdTe NPs

410 present on its surface and the second to the CdTe colloids with sizes from 165 to 340 nm. The

411 size distribution of particles separated from the ApoCdTe NPs solution by anchor system

412 shows that the apoferritin was modified by Au NPs and probably also attached to the Au NPs

413 clusters. The size distribution of particles attributed to apoferritin modified with CdTe NPs

414 and Au NPs was from 12 to 42 nm with the biggest intensity at 21 nm. We assume that the

415 thiolated oligonucleotide was still bound to the apoferritin and contributed to the peak shift.

416 Particles of size of 105 nm were also separated from ApoCdTe NPs solution, which suggests

417 that aggregated Au NPs were also anchored. Although the small overlap of CdTe NPs

418 colloids size distribution from ApoCdTe NPs sample and size distribution of particles

419 separated from ApoCdTe NPs sample was observed, we conclude that no CdTe NPs colloids

420 were anchored, because no fraction bigger than CdTe NPs colloids was observed in the size

421 distribution of anchored particles, which confirms the results from AAS measurement of the

422 control sample. The sample, where the highest concentration of cadmium was proven, was

423 also analysed by X-ray fluorescence (XRF). The measurement of XRF spectra confirmed the

424 presence of tellurium (the $L\alpha_1$ line energy corresponds to 3.134 keV and $L\beta_1$ to 3.317 keV)

425 and also cadmium (the $L\alpha_1$ corresponds to 3.769 keV and $L\beta_1$ to 4.030 keV) in the solution

426 containing ApoCdTe NPs (Fig. 3D).

427 We also tested the effect of CdTe NPs nanoparticles on the fluorescence of tryptophan in

428 apoferritin. The fluorescence spectra of ApoCdTe NPs sample were compared with the

429 spectra of CdTe NPs solution with added apoferritin. Apoferritin emissions in the presence of

430 cadmium, tellurite and ammonium ions were measured and subtracted from the emissions of

431 ApoCdTe NPs and mixture of CdTe NPs and apoferritin, which were monitored during

432 heating (20, 25, 30, 35, 40, 45, 50, 55 and 60 °C) using excitation wavelength 380 nm. This

433 excitation wavelength was chosen in order to observe changes in the apoferritin emission peak

434 width rather than emission maxima and to enable observing subtle changes of tryptophan

435 fluorescence. The addition of apoferritin to CdTe NPs solution resulted in complete

436 disappearance of CdTe NPs peak at 602 nm, which was replaced by the emission of

437 tryptophan at 450 nm (excitation wavelength 380 nm). The concentration dependent ability of

438 protein to quench different types CdTe quantum dots was previously described by Wang et al.

439 [72] and the mechanism of apoferritin interaction with CdTe NPs without surface stabilisation is

440 described by Stern-Volmer equation described above. In addition, we compared fluorescence

441 intensities of ApoCdTe NPs and apoferritin covered with CdTe NPs. In the case of both

442 samples, fluorescence of apoferritin tryptophan was statically quenched (fluorescence was

443 decreased) by the presence of CdTe NPs on apoferritin surface, whereas it was reported

444 previously that hydrous ferric oxides emerging at ferroxidase centres are able to quench

445 tryptophan fluorescence [73]. The increasing temperatures resulted in the growing and finally

446 aggregation of CdTe NPs and release of growing CdTe NPs from apoferritin surface and led

447 to the increase of apoferritin fluorescence (Fig. 3E), which is in good agreement with results

448 obtained by Chen et al. [74]. The total release was observed at 50 °C. After the release of CdTe

449 NPs from apoferritin surface, fluorescence of apoferritin with CdTe NPs within cavity was

450 still partly quenched (Fig. 3Eb). On the contrary, the fluorescence of apoferritin with CdTe

451 only on its surface was almost same as apoferritin control after heating.

452

453 **Figure 3**

454

455

4. Conclusions

Apoferritin is appealing molecule. Due to its inner cavity, it is extensively investigated as a nanoreactor or drug carrier. We designed the nanoconstruct, which is able to selectively bind apoferritin molecules modified by gold nanoparticles and separate them from solution of unreacted components and therefor to purify the required product. This simple anchor system enables to analyse the anchored molecule modification with target analyte, its degree or amount of encapsulated analyte. In order to test this concept we utilized apoferritin cavity as a nanoreactor and synthesized apoferritin modified by CdTe nanoparticles, which was proved to be presented on the surface and within apoferritin cavity.

471 **Captions for Figures**

472 **Figure 1**

473 Individual steps of CdTe NPs synthesis within apoferritin (ApoCdTe NPs) and their

474 characterization. (**A**) The scheme of the ApoCdTe NPs synthesis which was monitored using

475 UV-vis spectrometry and fluorescence spectroscopy and compared with control samples. The

476 absorption and fluorescence spectra of (**a**) apoferritin solution, (**b**) cadmium acetate,

477 ammonium and sodium tellurite water solution and (**c**) same mixture with addition of

478 apoferritin were measured (**B, C**) before reduction step, (**D, E**) after reduction and (**F, G**) after

479 heating. To highlight differences between ApoCdTe NPs and apoferritin sample the

480 differential (**H**) absorption and (**I**) fluorescence spectra (a) before reduction, (b) after

481 reduction and (c) after incubation were calculated. (**J**) To encourage CdTe creation heating is

482 required, thus apoferrtin thermostability was determined. The absorbance of apoferritin

483 solution at 230 nm during the heating depicted as percentages of decrease and (**K**) the native

484 PAGE of heated apoferritin solution to particular temperature. (**L**) The sizes distribution of

485 (**a**) CdTe colloids, (**b**) apoferritin in its spheric state and (**c**) particles presented within

486 ApoCdTe NPs sample. (**M**) Stern-Volmers K_{SV} constants were determined to elucidate

487 interaction mechanism between CdTe NPs by apoferritin at different temperatures.

488

489 **Figure 2**

490 Creation of anchor system. (**A**) The native PAGE shows the (**a**) apoferritin sample, (**b**) the

491 ApoCdTe NPs sample after heating, (**c** and **d**) the filtrate obtained by filtration of apoferritin

492 and ApoCdTe NPs sample through filter unit after heating, and (**e** and **f**) apoferritin and

493 ApoCdTe NPs sample after Au NPs modification. (**B**) The average current levels of

494 individual parts of nanoconstruct measured by SECM confirmed individual steps of anchor

495 system creation. (**C**) The image of ApoCdTe NPs anchored to magnetic particles obtained by

496 SECM.

497

498 **Figure 3**

499 Proving of apoferritin modification with CdTe NPs. (**A**) The scheme of ApoCdTe NPs

500 anchored to the separative nanoconstruct used to prove the dependence of detected cadmium

501 amount on the amount of anchored apoferritin (**B**). (**C**) The sizes of gold nanoparticles (**a**)

502 used for apoferritin modification, (**b**) particles presented within the ApoCdTe NPs sample and

503 (**c**) the particles separated by anchor system. (**D**) The XRF spectra shows that Cd and Te ions

504 were presented in ApoCdTe NPs sample separated by the anchor system. In inset: the photo

505 of water on the left and ApoCdTe NPs on the right side after excitation by 312 nm. (**E**) The

506 dependence of fluorescence on the heating temperature for (**a**) CdTe solution with apoferritin

507 added after CdTe synthesis, (**b**) ApoCdTe NPs and (**c**) the CdTe without any capping agent

508 suggests that portion of CdTe NPs is presented within apoferritin cavity.

509

References

1.   G. M. Whitesides, *Small*, 2005, **1**, 172-179.
2.   L. Sironi, S. Freddi, M. Caccia, P. Pozzi, L. Rossetti, P. Pallavicini, A. Dona, E. Cabrini, M. Gualtieri, I. Rivolta, A. Panariti, L. D'Alfonso, M. Collini and G. Chirico, *J. Phys. Chem. C*, 2012, **116**, 18407-18418.
3.   B. S. Yin, S. W. Zhang, Y. Jiao, Y. Liu, F. Y. Qu, Y. J. Ma and X. Wu, *J. Nanosci. Nanotechnol.*, 2014, **14**, 7157-7160.
4.   H. Zhang, S. S. Jia, M. Lv, J. Y. Shi, X. L. Zuo, S. Su, L. H. Wang, W. Huang, C. H. Fan and Q. Huang, *Anal. Chem.*, 2014, **86**, 4047-4051.
5.   G. D. Liu, H. Wu, J. Wang and Y. H. Lin, *Small*, 2006, **2**, 1139-1143.
6.   H. L. Li, Y. C. Zhu, S. G. Chen, O. Palchik, J. P. Xiong, Y. Koltypin, Y. Gofer and A. Gedanken, *J. Solid State Chem.*, 2003, **172**, 102-110.
7.   H. Y. Hsueh, H. Y. Chen, Y. C. Hung, Y. C. Ling, S. Gwo and R. M. Ho, *Adv. Mater.*, 2013, **25**, 1780-1786.
8.   W. Zhou, K. Zheng, L. He, R. M. Wang, L. Guo, C. P. Chen, X. Han and Z. Zhang, *Nano Lett.*, 2008, **8**, 1147-1152.
9.   K. Uto, K. Yamamoto, N. Kishimoto, M. Muraoka, T. Aoyagi and I. Yamashita, *J. Nanosci. Nanotechnol.*, 2014, **14**, 3193-3201.
10.   C. B. Mao, D. J. Solis, B. D. Reiss, S. T. Kottmann, R. Y. Sweeney, A. Hayhurst, G. Georgiou, B. Iverson and A. M. Belcher, *Science*, 2004, **303**, 213-217.
11.   S. Stefanini, S. Cavallo, C. Q. Wang, P. Tataseo, P. Vecchini, A. Giartosio and E. Chiancone, *Arch. Biochem. Biophys.*, 1996, **325**, 58-64.
12.   R. R. Crichton and C. F. A. Bryce, *Biochem. J.*, 1973, **133**, 289-299.
13.   M. Uchida, M. T. Klem, M. Allen, P. Suci, M. Flenniken, E. Gillitzer, Z. Varpness, L. O. Liepold, M. Young and T. Douglas, *Adv. Mater.*, 2007, **19**, 1025-1042.
14.   M. J. Parker, M. A. Allen, B. Ramsay, M. T. Klem, M. Young and T. Douglas, *Chem. Mat.*, 2008, **20**, 1541-1547.
15.   I. Yamashita, J. Hayashi and M. Hara, *Chem. Lett.*, 2004, **33**, 1158-1159.
16.   T. Ueno, M. Suzuki, T. Goto, T. Matsumoto, K. Nagayama and Y. Watanabe, *Angew. Chem.-Int. Edit.*, 2004, **43**, 2527-2530.
17.   R. Tsukamoto, K. Iwahori, M. Muraoka and I. Yamashita, *Abstr. Pap. Am. Chem. Soc.*, 2005, **229**, U938-U939.
18.   B. Hennequin, L. Turyanska, T. Ben, A. M. Beltran, S. I. Molina, M. Li, S. Mann, A. Patane and N. R. Thomas, *Adv. Mater.*, 2008, **20**, 3592-3596.
19.   T. D. Bradshaw, M. Junor, A. Patane, P. Clarke, N. R. Thomas, M. Li, S. Mann and L. Turyanska, *J. Mat. Chem. B*, 2013, **1**, 6254-6260.
20.   X. Y. Liu, W. Wei, S. J. Huang, S. S. Lin, X. Zhang, C. M. Zhang, Y. G. Du, G. H. Ma, M. Li, S. Mann and D. Ma, *J. Mat. Chem. B*, 2013, **1**, 3136-3143.
21.   K. L. Fan, L. Z. Gao and X. Y. Yan, *Wiley Interdiscip. Rev.-Nanomed. Nanobiotechnol.*, 2013, **5**, 287-298.
22.   E. Fantechi, C. Innocenti, M. Zanardelli, M. Fittipaldi, E. Falvo, M. Carbo, V. Shullani, L. D. Mannelli, C. Ghelardini, A. M. Ferretti, A. Ponti, C. Sangregorio and P. Ceci, *ACS Nano*, 2014, **8**, 4705-4719.
23.   I. Blazkova, H. V. Nguyen, S. Dostalova, P. Kopel, M. Stanisavljevic, M. Vaculovicova, M. Stiborova, T. Eckschlager, R. Kizek and V. Adam, *Int. J. Mol. Sci.*, 2013, **14**, 13391-13402.
24.   B. H. Jun, M. S. Noh, G. Kim, H. Kang, J. H. Kim, W. J. Chung, M. S. Kim, Y. K. Kim, M. H. Cho, D. H. Jeong and Y. S. Lee, *Anal. Biochem.*, 2009, **391**, 24-30.

Journal of Materials Chemistry B Accepted Manuscript

558 25. D. Huska, J. Hubalek, V. Adam, D. Vajtr, A. Horna, L. Trnkova, L. Havel and R.
559 Kizek, *Talanta*, 2009, **79**, 402-411.
560 26. J. H. Min, M. K. Woo, H. Y. Yoon, J. W. Jang, J. H. Wu, C. S. Lim and Y. K. Kim,
561 *Anal. Biochem.*, 2014, **447**, 114-118.
562 27. S. H. Lim, F. Bestvater, P. Buchy, S. Mardy and A. D. C. Yu, *Sensors*, 2009, **9**, 5590-
563 5599.
564 28. L. B. Nie, X. L. Wang, S. Li and H. Chen, *Anal. Sci.*, 2009, **25**, 1327-1331.
565 29. F. Patolsky, Y. Weizmann, E. Katz and I. Willner, *Angew. Chem.-Int. Edit.*, 2003, **42**,
566 2372-2376.
567 30. Y. S. Xing, P. Wang, Y. C. Zang, Y. Q. Ge, Q. H. Jin, J. L. Zhao, X. Xu, G. Q. Zhao
568 and H. J. Mao, *Analyst*, 2013, **138**, 3457-3462.
569 31. C. L. Cowles and X. S. Zhu, *Anal. Methods*, 2013, **5**, 801-804.
570 32. P. Hu, C. Z. Huang, Y. F. Li, J. Ling, Y. L. Liu, L. R. Fei and J. P. Xie, *Anal. Chem.*,
571 2008, **80**, 1819-1823.
572 33. X. L. Han, P. Mei, Y. Liu, Q. Xiao, F. L. Jiang and R. Li, *Spectroc. Acta Pt. A-Molec.*
573 *Biomolec. Spectr.*, 2009, **74**, 781-787.
574 34. J. Kimling, M. Maier, B. Okenve, V. Kotaidis, H. Ballot and A. Plech, *J. Phys. Chem.*
575 *B*, 2006, **110**, 15700-15707.
576 35. J. Polte, T. T. Ahner, F. Delissen, S. Sokolov, F. Emmerling, A. F. Thunemann and R.
577 Kraehnert, *J. Am. Chem. Soc.*, 2010, **132**, 1296-1301.
578 36. M. A. Kilic, S. Spiro and G. R. Moore, *Protein Sci.*, 2003, **12**, 1663-1674.
579 37. J. R. Lakowicz, *Principles of Fluorescence Spectroscopy*, Springer, New York, 2006.
580 38. Q. Xiao, H. N. Qiu, S. Huang, C. S. Huang, W. Su, B. Q. Hu and Y. Liu, *Mol. Biol.*
581 *Rep.*, 2013, **40**, 5781-5789.
582 39. T. Takahashi and S. Kuyucak, *Biophys. J.*, 2003, **84**, 2256-2263.
583 40. S. Aime, L. Frullano and S. G. Crich, *Angew. Chem.-Int. Edit.*, 2002, **41**, 1017-+.
584 41. K. Bartling, A. Sambanis and R. W. Rousseau, *Cryst. Growth Des.*, 2007, **7**, 569-575.
585 42. D. M. Lawson, P. J. Artymiuk, S. J. Yewdall, J. M. A. Smith, J. C. Livingstone, A.
586 Treffry, A. Luzzago, S. Levi, P. Arosio, G. Cesareni, C. D. Thomas, W. V. Shaw and
587 P. M. Harrison, *Nature*, 1991, **349**, 541-544.
588 43. A. Datta, S. Chatterjee, A. K. Sinha, S. N. Bhattacharyya and A. Saha, *J. Lumines.*,
589 2006, **121**, 553-560.
590 44. J. T. Vivian and P. R. Callis, *Biophys. J.*, 2001, **80**, 2093-2109.
591 45. A. Kowalska-Baron, K. Galecki, K. Rozniakowski, B. Kolesinska, Z. J. Kaminski and
592 S. Wysocki, *Spectroc. Acta Pt. A-Molec. Biomolec. Spectr.*, 2014, **128**, 830-837.
593 46. I. Yamashita, *Abstr. Pap. Am. Chem. Soc.*, 2005, **229**, U906-U906.
594 47. H. Y. Han, Z. H. Sheng and H. G. Liang, *Mater. Lett.*, 2006, **60**, 3782-3785.
595 48. Y. Khalavka, B. Mingler, G. Friedbacher, G. Okrepka, L. Shcherbak and O. Panchuk,
596 *Phys. Status Solidi A-Appl. Mat.*, 2010, **207**, 370-374.
597 49. K. K. W. Wong and S. Mann, *Adv. Mater.*, 1996, **8**, 928-&.
598 50. J. B. Xiao, Y. L. Bai, Y. F. Wang, J. W. Chen and X. L. Wei, *Spectroc. Acta Pt. A-*
599 *Molec. Biomolec. Spectr.*, 2010, **76**, 93-97.
600 51. J. Zhang, L. N. Chen, B. R. Zeng, Q. L. Kang and L. Z. Dai, *Spectroc. Acta Pt. A-*
601 *Molec. Biomolec. Spectr.*, 2013, **105**, 74-79.
602 52. H. Herberhold, S. Marchal, R. Lange, C. H. Scheyhing, R. F. Vogel and R. Winter, *J.*
603 *Mol. Biol.*, 2003, **330**, 1153-1164.
604 53. D. W. Yang, K. Matsubara, M. Yamaki, S. Ebina and K. Nagayama, *Biochim.*
605 *Biophys. Acta-Protein Struct. Molec. Enzym.*, 1994, **1206**, 173-179.
606 54. M. Weik and J. P. Colletier, *Acta Crystallogr. Sect. D-Biol. Crystallogr.*, 2010, **66**,
607 437-446.

55. H. Wu, S. H. Fan, H. Chen, J. Shen, Y. Y. Geng, L. Peng and H. L. Du, *Anal. Methods*, 2014, **6**, 4729-4733.

56. Z. Kriz, J. Klusak, Z. Kristofikova and J. Koca, *PLoS One*, 2013, **8**, 1-14.

57. R. Esfandiary, J. S. Hunjan, G. H. Lushington, S. B. Joshi and C. R. Middaugh, *Protein Sci.*, 2009, **18**, 2603-2614.

58. P. F. Liu, L. V. Avramova and C. Park, *Anal. Biochem.*, 2009, **389**, 165-170.

59. M. Giovanni and M. Pumera, *Electroanalysis*, 2012, **24**, 615-617.

60. Y. J. Hu, C. H. Chen, S. Zhou, A. M. Bai and Y. Ou-Yang, *Mol. Biol. Rep.*, 2012, **39**, 2781-2787.

61. M. Hossain, A. Y. Khan and G. S. Kumar, *PLoS One*, 2011, **6**, 1-12.

62. F. Li, H. Q. Zhang, B. Dever, X. F. Li and X. C. Le, *Bioconjugate Chem.*, 2013, **24**, 1790-1797.

63. B. L. V. Prasad, C. M. Sorensen and K. J. Klabunde, *Chem. Soc. Rev.*, 2008, **37**, 1871-1883.

64. A. Vallee, V. Humblot and C. M. Pradier, *Accounts Chem. Res.*, 2010, **43**, 1297-1306.

65. F. Y. Yeh, T. Y. Liu, I. H. Tseng, C. W. Yang, L. C. Lu and C. S. Lin, *Biosens. Bioelectron.*, 2014, **61**, 336-343.

66. R. Luo, Y. H. Li, X. J. Lin, F. Dong, W. Zhang, L. Yan, W. Cheng, H. X. Ju and S. J. Ding, *Sens. Actuator B-Chem.*, 2014, **198**, 87-93.

67. M. Pumera, M. Aldavert, C. Mills, A. Merkoci and S. Alegret, *Electrochim. Acta*, 2005, **50**, 3702-3707.

68. G. Tomoaia, P. T. Frangopol, O. Horovitz, L. D. Bobos, A. Mocanu and M. Tomoaia-Cotisel, *J. Nanosci. Nanotechnol.*, 2011, **11**, 7762-7770.

69. P. Arosio, T. G. Adelman and J. W. Drysdale, *J. Biol. Chem.*, 1978, **253**, 4451-4458.

70. J. W. Kim, A. E. Posey, G. D. Watt, S. H. Choi and P. T. Lillehei, *J. Nanosci. Nanotechnol.*, 2010, **10**, 1771-1777.

71. M. A. Kilic, E. Ozlu and S. Calis, *J. Biomed. Nanotechnol.*, 2012, **8**, 508-514.

72. S. S. Wang, X. T. Wang, M. M. Guo and J. S. Yu, *Chem. J. Chin. Univ.-Chin.*, 2012, **33**, 1195-1204.

73. F. Bou-Abdallah, G. Zhao, G. Biasiotto, M. Poli, P. Arosio and N. D. Chasteen, *J. Am. Chem. Soc.*, 2008, **130**, 17801-17811.

74. M. Shen, W. P. Jia, Y. J. You, Y. Hu, F. Li, S. D. Tian, J. Li, Y. X. Jin and D. M. Han, *Nanoscale Res. Lett.*, 2013, **8**, 1-6.
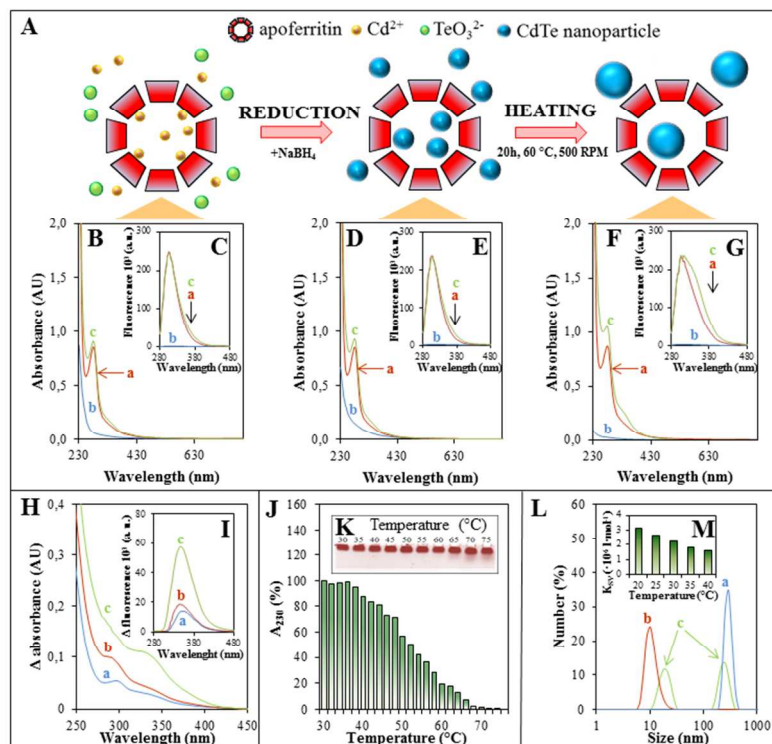
Figure 1

Individual steps of CdTe NPs synthesis within apoferritin (ApoCdTe NPs) and their characterization. (A) The scheme of the ApoCdTe NPs synthesis which was monitored using UV-vis spectrometry and fluorescence spectroscopy and compared with control samples. The absorption and fluorescence spectra of (a) apoferritin solution, (b) cadmium acetate, ammonium and sodium tellurite water solution and (c) same mixture with addition of apoferritin were measured (B, C) before reduction step, (D, E) after reduction and (F, G) after heating. To highlight differences between ApoCdTe NPs and apoferritin sample the differential (H) absorption and (I) fluorescence spectra (a) before reduction, (b) after reduction and (c) after incubation were calculated. (J) To encourage CdTe creation heating is required, thus apoferrtin thermostability was determined. The absorbance of apoferritin solution at 230 nm during the heating depicted as percentages of decrease and (K) the native PAGE of heated apoferritin solution to particular temperature. (L) The sizes distribution of (a) CdTe colloids, (b) apoferritin in its spheric state and (c) particles presented within ApoCdTe NPs sample. (M) Stern-Volmers KSV constants were determined to elucidate interaction mechanism between CdTe NPs by apoferritin at different temperatures.
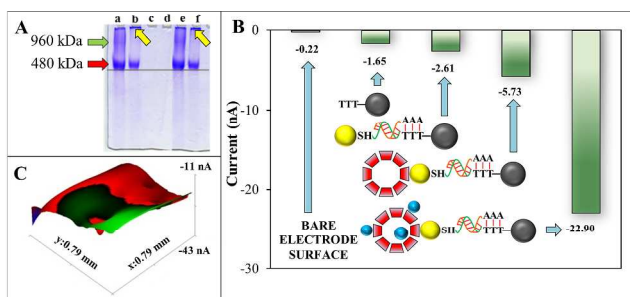
Figure 2

Creation of anchor system. (A) The native PAGE shows the (a) apoferritin sample, (b) the ApoCdTe NPs sample after heating, (c and d) the filtrate obtained by filtration of apoferritin and ApoCdTe NPs sample through filter unit after heating, and (e and f) apoferritin and ApoCdTe NPs sample after Au NPs modification. (B) The average current levels of individual parts of nanoconstruct measured by SECM confirmed individual steps of anchor system creation. (C) The image of ApoCdTe NPs anchored to magnetic particles obtained by SECM.
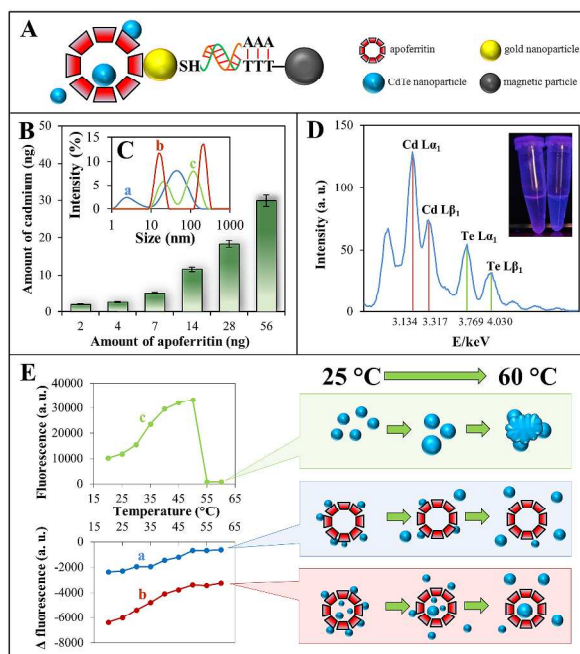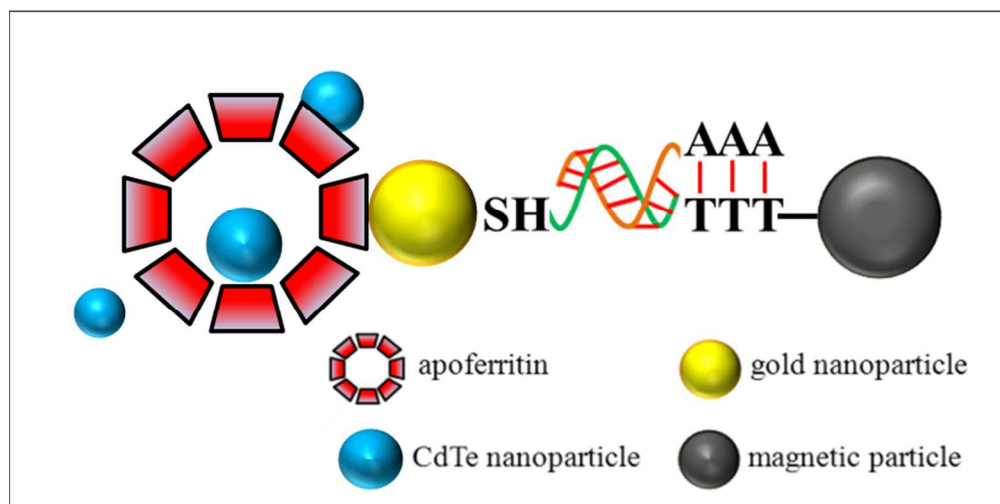
Figure 3

Proving of apoferritin modification with CdTe NPs. (A) The scheme of ApoCdTe NPs anchored to the separative nanoconstruct used to prove the dependence of detected cadmium amount on the amount of anchored apoferritin (B). (C) The sizes of gold nanoparticles (a) used for apoferritin modification, (b) particles presented within the ApoCdTe NPs sample and (c) the particles separated by anchor system. (D) The XRF spectra shows that Cd and Te ions were presented in ApoCdTe NPs sample separated by the anchor system. In inset: the photo of water on the left and ApoCdTe NPs on the right side after excitation by 312 nm. (E) The dependence of fluorescence on the heating temperature for (a) CdTe solution with apoferritin added after CdTe synthesis, (b) ApoCdTe NPs and (c) the CdTe without any capping agent suggests that portion of CdTe NPs is presented within apoferritin cavity.

Journal of Materials Chemistry B

79x39mm (300 x 300 DPI)